

Recent Progress in Polymeric Flexible Surface Acoustic Wave Devices: Materials, Processing, and Applications

Leonardo Lamanna

Recently, there has been a remarkable increase in interest in piezoelectric thin films, particularly zinc oxide (ZnO) and aluminum nitride (AlN), deposited on flexible polymeric substrates. This is due to the rapid expansion of fields such as robotics, wearable devices, and the Internet of Things (IoT). These thin-film layered structures have a wide range of applications, such as energy harvesting, sensing and biosensing, microfluidic sorting, pumping and mixing, and telecommunications. One of the most promising platforms is piezoelectric acoustic-based thin-film devices on inexpensive, recyclable, or disposable polymeric substrates. Their reliability, reproducibility, conformability, small size, and wireless control capabilities make them a leading candidate for the development of new wireless, fully automated, and digitized microsystems for IoT and wearable devices. This review examines recent advancements in the engineering of ZnO and AlN thin films on polymeric, flexible, and conformable surface acoustic wave (SAW) devices. Topics covered include the materials used, piezoelectric film deposition, device fabrication, and the latest applications of this technology as sensors and actuators.

wearable, and even edible devices.^[4,5] However, this review will focus specifically on recent advancements in flexible piezoelectric surface acoustic devices (SAW) fabricated on polymeric substrates.

Surface acoustic wave (SAW) thin film devices rely on wave propagation in piezoelectric films, making them a crucial component in micro-electro-mechanical-systems (MEMS) due to their low cost, low power consumption, and remote control capabilities.^[6–12] The piezoelectric film is deposited directly onto the substrate, allowing for easy integration with other electronic systems. The development of thin substrates, including silicon, glass, and metal, paved the way for the creation of the first flexible SAW devices based on such substrates.^[13,14] However, the use of such substrate leads to the production of fragile devices with limited flexibility and poor applicability

1. Introduction and Fundamentals of SAW


Flexibility in electronics is achieved through double lacing with a reduction in material thickness. The advent of thin circuits and substrates, such as silicon and glass, paved the way for the development of flexible electronics.^[1,2] This field has continued to grow and evolve, derived by advancements in high-performing polymers with high-temperature resistance and robust mechanical properties. These materials enable the integration of crystalline components with plastic substrates, further advancing the concept of flexible electronics.^[3] Today, the scope of flexible electronics is vast, ranging from integrated circuits to implantable,

in wearable applications, as well as being costly. Recently, polymeric substrates have also been investigated as potential substrates for these devices.^[15,16]

The use of polymeric substrates in the development of SAW devices has significant potential for creating environmentally friendly devices. The ability to recycle, degrade or dispose of the devices after use can significantly reduce the environmental impact associated with traditional devices.^[17,18] Additionally, the use of polymeric substrates allows for the development of compliant devices that can be used for wearable device applications, such as health monitoring and fitness tracking. This opens up a range of new possibilities for integrating SAW devices with other flexible electronic systems, such as OFET, OLED power source and communication systems, to create more and more advanced systems.^[5,19–22] While the research in this area is ongoing, significant progress has been made in recent years, and the future looks promising for the continued development and advancement of polymeric SAW devices. **Figure 1** provides an illustration of the topics covered in the review.

Among piezoelectric materials, Zinc Oxide (ZnO) and Aluminum Nitride (AlN) are the only materials used in polymeric SAW devices so far. Lead zirconate titanate (PZT) is excluded due to its toxicity, complex fabrication process, high annealing temperature, high electric field polarization, and incompatibility with complementary metal–oxide–semiconductor (CMOS) processes.^[23] This review will focus the attention mainly on polymeric SAW devices based on ZnO and AlN.

L. Lamanna
Department of Engineering for Innovation
Campus Ecotekne
University of Salento
Via per Monteroni, Lecce 73100, Italy
E-mail: leonardo.lamanna@unisalento.it

 The ORCID identification number(s) for the author(s) of this article can be found under <https://doi.org/10.1002/admt.202300362>

© 2023 The Authors. Advanced Materials Technologies published by Wiley-VCH GmbH. This is an open access article under the terms of the Creative Commons Attribution License, which permits use, distribution and reproduction in any medium, provided the original work is properly cited.

DOI: 10.1002/admt.202300362

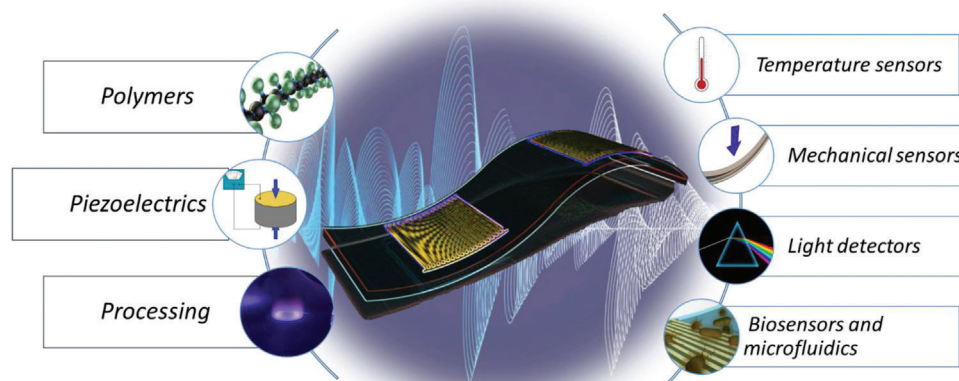


Figure 1. The illustration provides an overview of the topics covered in the review on polymeric surface acoustic wave (SAW) devices. The review delves into the challenges and latest developments in materials (polymers and piezoelectrics) and processing, examines the material properties of polymeric substrates and piezoelectric films, explores the results obtained with flexible SAW devices in various applications such as temperature, mechanical, light, and biosensing, and discusses future trends and potential breakthroughs in the field.

SAW devices exploit the propagation of traveling waves generated by applying an alternating current (AC) or radiofrequency (RF) excitation to electrodes patterned on the piezoelectric film, which generates a time-dependent deformation leading the propagation of such waves in/on the surface of the material. The SAW resonant frequency is related to the pattern of the electrode (λ) and the acoustic velocity in the piezoelectric film:

$$f_0 = \frac{c}{\lambda} \quad (1)$$

f_0 describe the resonance frequency where there is the maximum electromechanical transduction from the AC signal to the mechanical wave; c is the wave velocity that depends on the substrate's nature and kind of traveling wave.

In the polymeric SAW devices, two main wave modes of propagation are reported: Rayleigh (R-SAWs) at low frequency and Lamb wave (L-SAW) at high frequency (Figure 2a). R-SAWs are a combination of both longitudinal and transverse vibrations generating an elliptical retrograde motion in the vertical plane along the direction of travel. R-SAWs decrease rapidly with depth, such waves are defined as pure superficial waves.^[24,25] The R-SAW phase velocity is defined as:

$$c = \sqrt{\frac{E}{2(1+\nu)\rho}} \quad (2)$$

where E is Young's modulus, ν the Poisson ratio, and ρ the density of the piezoelectric film.

L-SAWs usually are generated when the substrate thickness is smaller than or comparable to the wavelength. Lamb waves are not strictly defined as SAWs, as they differ in their mode of propagation. They are more accurately described as plate waves that propagate in thin plates or membranes, where their velocity is dependent on the material's mechanical properties, thickness of the piezoelectric layer, and device design. Lamb waves typically have two modes of propagation: symmetric and anti-symmetric (Figure 1a), and own higher phase velocity with respect to R-

SAW.^[26] For the L-SAW symmetric and anti-symmetrical the phase velocities are defined as:^[23,27]

$$c_{\text{symmetric}} = \sqrt{\frac{E}{(1-\nu^2)\rho}} \quad (3)$$

$$c_{\text{anti-symmetric}} = \frac{2\pi h}{\lambda} \sqrt{\frac{E}{12(1-\nu^2)\rho} \frac{1}{\sqrt{\frac{\pi^2 h^2}{3\lambda^2} + 1}}} \quad (4)$$

where h defines the thickness of the membrane. L-SAWs are allowed in thin films grown on polymeric flexible substrates due to the softness of the polymer that does not oppose the vibrations of the piezoelectric layer.^[27,28]

The success of SAW devices is coming mainly from the reliability, sensitivity, and versatility, in fact, the wave velocity can depend on the material properties itself and the experimental/environmental conditions such as temperature ΔT , density $\Delta \sigma$, mass load Δm , dielectric constant $\Delta \epsilon$, viscosity $\Delta \eta$ perturbation.

$$\frac{\Delta v}{f_0} = \frac{\Delta v}{v_{\text{acoustic}}} = \frac{1}{v} \left(\frac{\partial v}{\partial T} \Delta T + \frac{\partial v}{\partial \sigma} \Delta \sigma + \frac{\partial v}{\partial m} \Delta m + \frac{\partial v}{\partial \epsilon} \Delta \epsilon + \frac{\partial v}{\partial \eta} \Delta \eta + \dots \right) \quad (5)$$

The sensitivity of SAW devices to an external stimulus x can be expressed as:

$$\text{SAW device}_{\text{sensitivity}} = \lim_{\Delta x \rightarrow 0} \frac{\Delta f}{\Delta x} = \frac{df}{fdx} \quad (6)$$

where Δf is the resonance shift due to the Δx variation, which represents the theoretical or experimental variation of λ . The variation is typically theoretical in the case of UV, mass, and viscosity sensitivity. However, for temperature and strain sensitivity, the variation is attributed to the thermal expansion coefficient and strain itself. It is important to note that material properties and

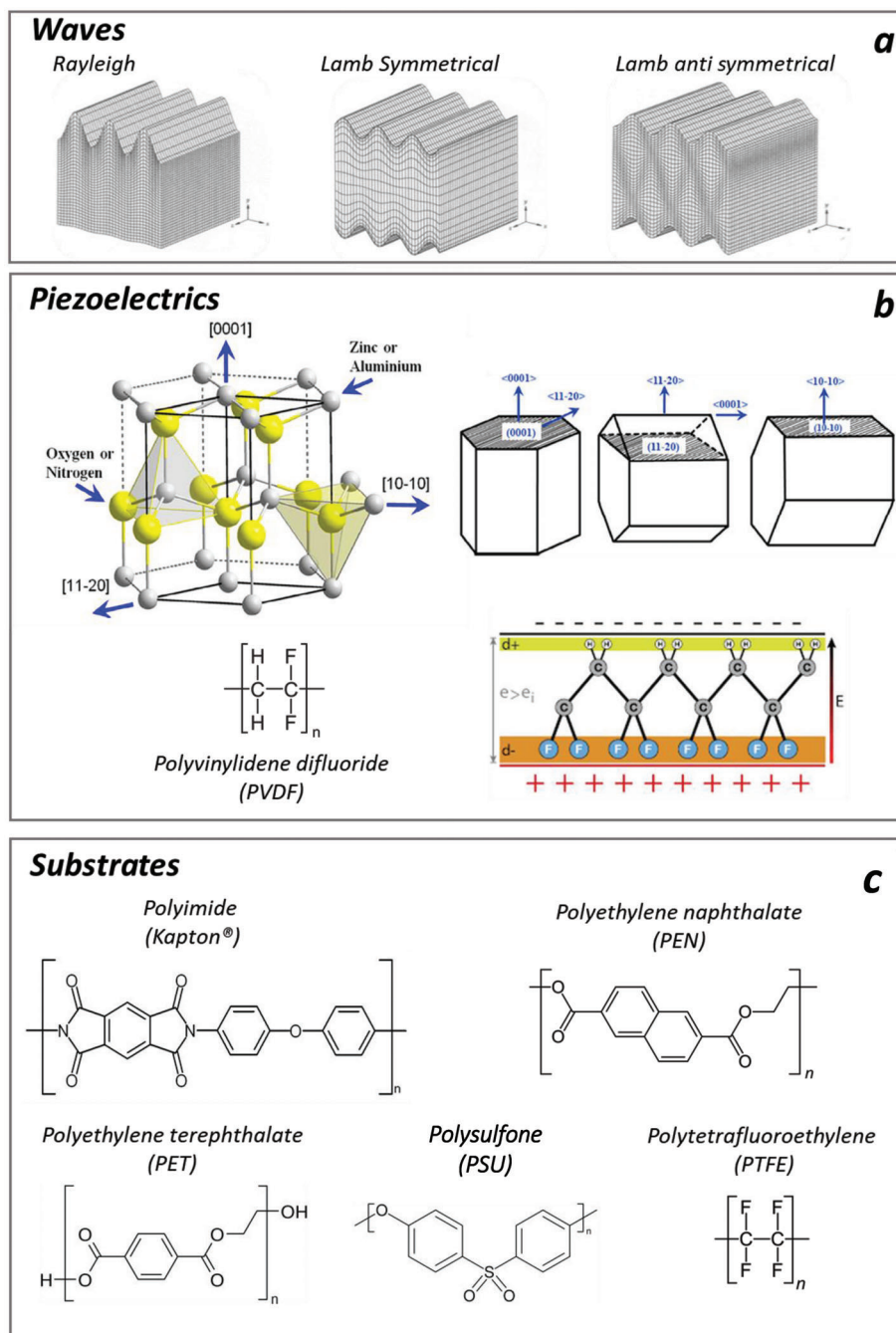


Figure 2. a) Main wave modes propagation reported in flexible polymeric SAW devices. Reproduced with permission.^[64] Copyright 2011, Wiley-VCH GmbH. b) Illustration of ZnO and AlN wurtzite crystal structures and PVDF molecular structure and piezoelectric beta phase. Reproduced with permission.^[23] Copyright 2017, Elsevier. c) Molecular structures of thermoset and thermoplastic polymer used in the development of flexible polymeric SAW devices.

fabrication techniques may also affect the actual device performance. When the SAW device is used as a mass loading sensor the frequency shift can be usually defined as:

$$\Delta f = \frac{2\Delta m f_0^2}{A\sqrt{\mu\rho}} \quad (7)$$

where μ is the ratio between mass and area, ρ is the density and A is the surface area. The sensitivity is typically proportional to the mass per unit area and square of the operating frequency (f_0).^[29]

The review will provide a comprehensive overview of the challenges and state-of-the-art in the development of polymeric surface acoustic wave (SAW) devices. The review will begin with a description of the materials used for polymeric substrates, as well

as the deposition of piezoelectric material onto these substrates. Despite significant advances in the field, the deposition of piezoelectric crystalline films on polymeric substrates remains a major bottleneck in the development of high-performing and reliable flexible SAW devices. This is due to the significant differences in the mechanical and thermal properties of these two layers, which present a significant challenge to device fabrication. This review will examine the properties of both polymeric substrates and piezoelectric films, highlighting the best combinations and strategies to date for achieving the desired results. By providing a comprehensive overview of the current state-of-the-art, serving as a resource for researchers working in the field of polymeric SAW devices.

In the second part of the review, the reader will find a detailed description of the results obtained with flexible polymeric SAW devices. Specifically, the review will explore four main pillars by analyzing the results that researchers have reported in the development of temperature sensors, mechanical sensors, light detectors, biosensors, and microfluidics based on polymeric SAW devices. Each of these areas will be discussed, highlighting the strengths and limitations of existing devices, as well as areas for future research and development.

In the last part of the review, prospective trends in the field of polymeric and flexible SAW devices will be proposed. The review will discuss the most promising avenues for future research and development, as well as potential applications for these devices in emerging fields such as wearable electronics and the Internet of Things.

2. Materials

The most used materials for the development of thin film SAW devices on polymeric substrates are ZnO and AlN. Despite efforts to develop a fully organic SAW device using polyvinylidene fluoride (PVDF), the material has not yet been successful. The low electro-mechanical coupling and low phase velocity of PVDF have prevented the fabrication of a functional SAW device. However, research in this area has continued.^[23,30–32] In the 1980s, Wager was the first to demonstrate SAW propagation on PVDF films at low temperatures ($-175\text{ }^{\circ}\text{C}$), but the high insertion loss and low temperature requirements limited its practical applications.^[33,34] In a subsequent study, Kumar et al. showed proof-of-concept for a PVDF-based SAW device with a resonating electrode configuration in both vertical and longitudinal directions. However, the SAW response was only demonstrated on PVDF deposited on glass.^[35] More recently, Govindarajan et al. proposed the development of a PVDF-based SAW device by adding micro/nano ceramic fillers such as lead zirconate titanate (PZT), calcium copper titanate (CCTO), and carbon nanotubes (CNTs), resulting in a device that operates around 50 MHz, but again, only on a steel substrate (Table 1).^[36]

2.1. ZnO

ZnO is an inorganic compound widely used as an additive in many compounds from plastic and cement. It is an n-type semiconductor of the II-VI group with high electron mobility.^[37] In

Table 1. Comparison of piezoelectric material exploited for the development of flexible polymeric SAW devices.

| Index | AlN | ZnO | PVDF |
|------------------------------------------|-------------|-----------|-----------|
| Young modulus (GPa) | 280–400 | 100–150 | 2–4 |
| Poisson's ratio | 0.22–0.29 | 0.35 | 0.33–0.4 |
| Density | 3–3.5 | 5.5–5.8 | 1.6–1.8 |
| R-SAW velocity (m/s) | 5000–6000 | 2400–3000 | 2500–2800 |
| L-SAW velocity (m/s) | 10000–12000 | 6000–8000 | – |
| Curie Temperature ($^{\circ}\text{C}$) | 800–1200 | 450–550 | 100–200 |
| D_{33} (pC/N) | 10–14 | 3–8 | –20 – –30 |

piezoelectric material hexagonal wurtzite structure is necessary, in which Zn^{2+} cation is surrounded by four O^{2-} and vice versa, generating a non-centrosymmetric arrangement, generating its piezoelectricity (Figure 2b). ZnO is a material widely used in electronic, optoelectronics, acoustic, and sensing applications thanks to its semiconductor, piezoelectric, and optical properties.^[38] ZnO-based polymeric SAW devices were the first to be developed due to the higher controllability of the ZnO deposition process. Moreover, good film crystallinity has been obtained at low temperatures.^[39] In fact, ZnO has low tensile residual stress and good adhesion to many substrates, allowing the deposition of up to tens of microns. On the contrary, ZnO owns low wave velocity with respect to AlN avoiding the development of high-frequency devices.^[40] Another advantage of ZnO is the possibility to develop nanostructure (e.g. nanowire/nanorods) on the top of the device that can be exploited for sensing applications.^[41,42]

The main drawback of ZnO is its high reactivity; in fact, the material is unstable if exposed to water or humidity for a long time. Moreover, Zn is considered a contaminant in the CMOS process, and it is incompatible with a process such as cryopumps.^[23,43] This constraint will limit the development of wearable sensors or sensors intended for use in water-based environments, as they will require a protective coating layer to prevent degradation of the ZnO over time.

2.2. AlN

Aluminum nitride inorganic salt of Al with a wide band gap ($\approx 6\text{ eV}$), high resistivity ($\approx 10^{12}\text{ }\Omega\text{ cm}$), and thermal conductivity $\approx 200\text{ W (m K)}$.^[44] AlN is exploited mainly in its wurtzite crystal structure, where Al and N alternate along the c-axis and each bond is tetrahedrally coordinated with four atoms per unit cell, generating a spontaneous polarization, and piezoelectric polarization (Figure 2b).

AlN owns high mechanical properties (e.g., young modulus) and can sustain high temperatures of $700\text{--}1000\text{ }^{\circ}\text{C}$,^[45] moreover, AlN deposition and processing is fully compatible with CMOS processes.^[43] Their crystalline and mechanical properties allow the propagation of high wave velocity, enabling the development of SAW devices operating at higher frequencies and higher powers, with improved sensitivity and performance at high temperatures.^[23] On the contrary, the deposition of AlN piezoelectric films is difficult to control and usually sputtered at elevated temperatures ($>200\text{ }^{\circ}\text{C}$), such film often owns high residual tensile stress. Moreover, moisture and oxygen

Table 2. Comparison of common polymeric substrate exploited for flexible SAW devices.

| | PI | PEN | PET | PES | PTFE |
|--------------------------------------------------|-------------------------------|---------|-----------|---------|-------------------------------|
| Thermal Coefficient of Linear Expansion (ppm/°C) | 20 | 20–21 | 50–92 | 55–90 | 80–135 |
| Glass Transition Temperature (°C) | 360–410 (not real transition) | 120–200 | 90–110 | 200–250 | 120–327 (not real transition) |
| Young modulus (GPa) | 2–4 | 5 | 2.1 | 4.8 | 0.5 |
| Poisson's ratio | 0.34 | 0.33 | 0.33–0.35 | 0.37 | 0.36–0.46 |
| Dielectric Constant | 3.4 | 3.2 | 3.6 | 3.17 | 2 |

contamination in the deposition chamber strongly affect the AlN growth and microstructure. Finally, AlN microstructures are not easy to produce and are not widely used for biosensing.^[46]

2.3. Polymers

To enable the development of flexible SAW devices, the polymeric substrate needs to have some key future such as resistance to temperature, solvents, and acids, low surface roughness, high mechanical properties, and low price. Resistance to the temperature is necessary to sustain the deposition of piezoelectric material that usually is lead to an increase in the temperature. Glass transition and high thermal expansion in the range of deposition temperature are not compatible with the growth of a homogeneous piezoelectric layer necessary for the SAW device fabrication. In general, the large mismatch in thermal expansion coefficients between the substrates and the piezoelectric films generates non-continuous, non-uniform, or amorphous crystal deposition. The resistance to solvent and/or acid is necessary for the post-processing, in fact, the fabrication of SAW devices usually needs photolithography, which requires exposing the material to solvents and acids. The substrate morphology represents the first imprinting to the piezoelectric deposition SAW devices the roughness is a key parameter influencing the propagation of the waves.^[47] In fact, SAWs propagate along the surface confining most of the energy within a wavelength from the surface, thus a low surface roughness is essential to avoid the acoustic wave dissipation.^[48] Lastly, the polymeric mechanical features are important; a large mismatching with the piezoelectric material leads to a significant attenuation and dissipation of acoustic energy in the plastic, forcing the increasing thickness of the piezoelectric layer (Table 2).

Both thermoset and thermoplastic materials have been exploited in the development of polymeric flexible SAW devices (chemical structures are reported in Figure 2c. Polyimide (PI) was the first candidate in the development of such MEMS. PIs are thermosetting polymers with typical orange/yellow color and are well known for their thermal stability, chemical resistance, and excellent mechanical properties. Commercial Kapton® de-

veloped by DuPont in the 1960s is the most common and widely exploited. Kapton® is a high-performance polymer that is known for its excellent thermal properties. It has a thermal coefficient of linear expansion (TCLE) as low as 20 ppm/°C, which means that its dimensions change very little with temperature fluctuations. TCLE is a measure of how much a material's length changes with temperature, and a low TCLE value indicates that a material is highly stable over a wide range of temperatures. In addition, Kapton® has a glass transition temperature (T_g) greater than 360 °C, which is the temperature at which a polymer transitions from a rigid, glass-like state to a rubbery, flexible state. For these feature PIs are commonly used in flexible and printed electronics; moreover, is used as space blankets on spacecraft and satellites.^[49,50]

PET and PEN are thermoplastic polymers representing a second and third evolution of polyethylene, where the addition of one and two aromatic rings respectively, generate an improvement in strength and modulus, chemical and hydrolytic resistance, gaseous barrier, thermal and thermo-oxidative resistance, and UV light barrier resistance.^[49] In particular, it is worth noting that PET and PEN have a T_g in the range of 90–110 and 120–200 °C, respectively. Furthermore, their coefficient of thermal expansion (TCLE) falls within the range of 50–92 and 20–21 ppm/°C for PET and PEN, respectively. These polymers represent more than 20% of the world's polymer production and are commonly recycled.

Polysulfones (PSU) are thermoplastic materials with high mechanical and thermal performances. They have T_g at temperature >200 °C and mechanical properties comparable with the PI. The main drawback is the high cost of processing with respect to other thermoplastic materials, however, the cost is offset by their ease of processing, durability, and design flexibility.^[50,51]

Polytetrafluoroethylene (PTFE) is a fluoropolymer, classified within the thermoplastic polymers, commercially known as Teflon. The strong C–F bond does not lead PTFE to react with any other compounds. PTFE owns high mechanical strength, hydrophobicity, chemical, and thermal stability. In fact, even at T_g temperature (>200 °C), PTFE does not flow and interact with any solvent.^[52] The main drawback of PTFE is the low adhesion and its environmental toxicity coming from both the manufacturing process and the end life of the plastic since such material is difficult to recycle and does not undergo any degradation.^[53]

3. Processing of Piezoelectric Material for Polymeric SAW Devices

In literature, many methods have been reported to deposit ZnO and AlN films including physical vapor deposition (PVD), such as sputtering,^[54–56] evaporation,^[57] pulsed laser deposition (PLD),^[58,59] molecular beam epitaxy (MBE),^[60,61] chemical vapor deposition (CVD).^[62,63] Different deposition processes lead to different crystalline quality, temperature, costs, and rates of deposition. Among all the techniques, magnetron sputtering is the only one exploited for the development of SAW devices on the polymeric substrate because of its, simplicity, good reproducibility, operating temperature, and compatibility with MEMS processing. Films of ZnO and AlN are deposited on polymeric substrates with DC/RF sputtering at room/low temperature, using high purity Zn and Al targets in Ar and O₂ or N₂ gas mixture, or using RF sputtering and ceramic ZnO or AlN target (Figure 3a).

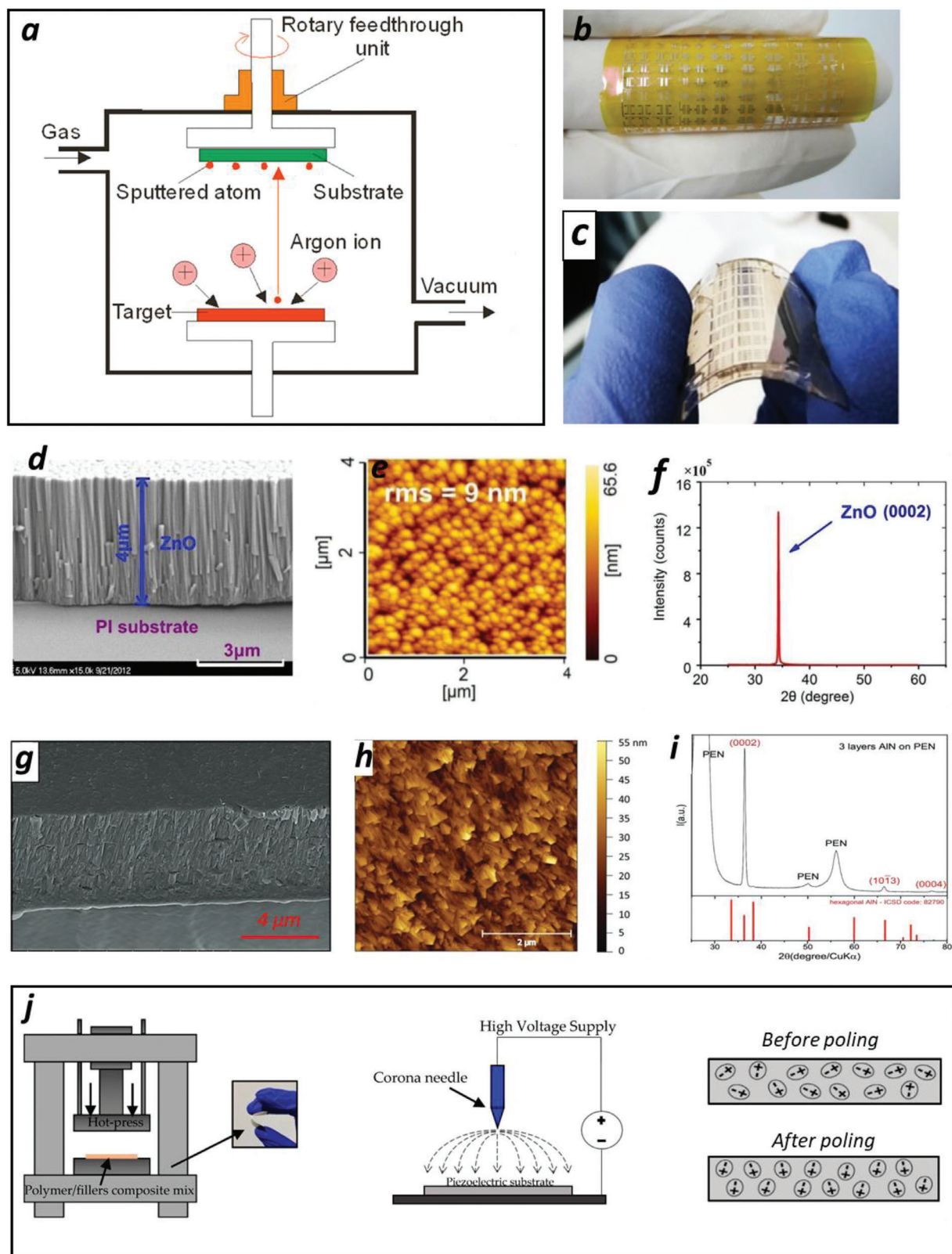


Figure 3. a) Illustration of a sputtering deposition process; b,c) Photographs of flexible polymeric SAW devices that are based on ZnO/PI and AlN/PEN respectively; d) Characterization of ZnO deposited on PI: SEM, AFM, and XRD. Reproduced with permission.^[16] Copyright 2013, Springer Nature. f) Similarly, AlN deposited on PEN is characterized through SEM, AFM, and XRD. Reproduced with permission.^[15] Copyright 2019, Wiley-VCH GmbH. j) Processing of PVDF piezoelectric film: hot-pressed thin sample and schematic of corona poling with dipole orientation before and after poling. Reproduced under the term of CC-BY license.^[36] Copyright 2021, The Authors, published by MDPI.

The propagation of the SAWs is lead to the generation of polar wurtzite structure of ZnO and AlN with a crystal orientation in c-axis that show the highest piezoelectric constant d_{33} . The thickness of the piezoelectric layer is crucial for the design of a flexible SAW device; a lower h/λ ratio brings stronger damping due to the large mismatch of the mechanical properties between the ceramic and the polymeric layers.^[23,65] In general, SAW devices usually need a piezoelectric layer whose thickness should be larger than 10% of the acoustic wavelength, such ratio should be increased in the polymeric substrate due to the high mechanical mismatching between the substrate and the piezoelectric layer. To achieve such thickness, the process of deposition became longer with a consequent increase of temperature in the chamber, making the deposition on polymeric substrate challenging. To avoid such temperature increases, chillers or multistep deposition processes have been developed.^[15,66]

Different doping elements (e.g., P, As, Sb, CA, Sr, Ga) have been exploited to modify piezoelectric and dielectric properties, as well as energy band gap and optical features of ZnO and AlN films.^[67–69] Although the doping of ZnO and AlN have been investigated on the feature of the conventional, rigid acoustic devices, to date no reports are present on such doped film on polymeric SAW devices. The cause is to be addressed to the non-uniform distribution and reproducibility, and current research is based on “*trial and error*”.^[70]

Polymeric SAW devices based on ZnO were the first to be developed. ZnO has been successfully deposited on PI substrate obtaining highly-oriented columnar nano grains perpendicular to the polymeric film.^[71,72] Jin et al. after the deposition of 4 μm measured a root mean square (RMS) roughness of 9 nm over an area of $4 \times 4 \mu\text{m}^2$, comparable to those obtained from the films deposited on solid substrates (Figure 3b–e).^[32,33] Detailed sputtering deposition characterization of ZnO on PI is reported by Zhou et al., where the authors have analyzed the ZnO crystalline structure in relation to thickness, deposition rate, power, bias voltage, and gas pressure.^[71] Deposition from 3.5 to 4.5 μm of ZnO has been successfully obtained even on PET at temperatures below 120 °C, with high 0002 crystal orientation.^[73] Other polymers such as Polyethersulfone (PES),^[74,75] Benzocyclobutene (BCB),^[76] and fluoropolymers such as (PTFE-HFP)^[76–78] have been investigated as substrates for ZnO deposition. However, no flexible SAW devices based on these substrates are reported, probably due to the higher TCLE that avoids the deposition of the thick piezoelectric layer necessary for wave propagation.

Similarly, but limited in scientific reports is the state of the art on the deposition of AlN on polymeric substrates, which is reported mainly on PI and PEN. As previously discussed, the deposition of piezoelectric AlN is more challenging requiring high temperature and tight control of the deposition parameters. PI is the first and most reported substrate in the deposition of flexible piezoelectric AlN MEMS.^[79–81] In particular, Algieri et al. reported deposition of a columnar of 0002-oriented AlN with a minimum RMS 6.32 nm on an area of $5 \times 5 \mu\text{m}$ and a d_{33} of 4.93 pm V^{-1} .^[81] The first report of the SAW device based on PI/AlN was developed by Zhou et al.^[82] with a low transmission amplitude (<1db). Li et al. recently developed a SAW device with AlN working at 4.95 GHz, improving the piezoelectric response

(8.01 pm V^{-1}) and reducing the roughness (3.2 nm) by adding a molybdenum interlayer of 200 nm.^[83]

PEN has demonstrated, thanks to its thermal resistance and low surface roughness, superior capability to sustain the deposition process of AlN, and the development of SAW device.^[15,84,85] Lamanna et al. have reported a multilayer AlN deposition on PEN, allowing the increase of thickness, keeping as low as possible the deposition temperature.^[15] The multistep deposition has allowed the development of 4.5 μm thick AlN with c-oriented columnar growth RMS of 8.04 nm, an average grain size of 49 nm, and d_{33} of 3.29 pm V^{-1} ^[15] (Figure 3c,g–i). The device fabricated with this substrate showed a transmission amplitude as high as 22 dB.

PVDF is generally synthesized by free radical polymerization of difluoroethylene, followed by processes such as melt casting, solution casting, and spin coating. The obtained material is usually in a non-piezoelectric alpha phase, which needs to be stretched/annealed/poled to obtain the piezoelectric beta phase. The poling process under a large electric field (tens MV/m), eventually in a temperature range between 70–100 °C, is commonly reported to generate piezoelectric films.^[86–88] The only example of a SAW device based on PVDF composite was presented recently by Govindarajan et al.^[90] The authors dissolved/dispersed PVDF with different ceramic nanofillers in DMSO, and hot pressed at 179 °C (melting temperature of PVDF) for 20 min. Subsequently, the film where electrically polarized, to generate the beta phase in a non-contact method (corona pooling) with a voltage ff 12–15 kV at 2–3 cm for 30 min (Figure 3j)

4. Applications

The development of polymeric flexible SAW devices has unlocked a multitude of opportunities in the field of the Internet of Things (IoT) and healthcare. Their exceptional conformability, low power consumption, remote control capability, and sensitivity to a range of environmental conditions make them an ideal solution for low-power sensing and communication applications. In this section, we will provide an overview of the various sensing and actuation applications of polymeric SAW devices and demonstrate their potential to revolutionize the IoT and healthcare sectors.

4.1. Temperature Sensors

Acoustic wave velocity propagation depends on temperature, for this reason, such an effect can be exploited for the development of temperature sensors. The temperature coefficient of frequency describes the sensitivity of SAW devices to the temperature.

$$\text{TCF} = \frac{\Delta f}{\Delta T f_0} \quad (8)$$

Δf represents the frequency variation driven by the temperature variation (ΔT) and f_0 is the resonance frequency at 25 °C. Values of the TCFs are influenced by substrates, piezoelectric, and working device frequency. Polymeric-based SAW devices are more influenced by temperature, with respect to standard rigid

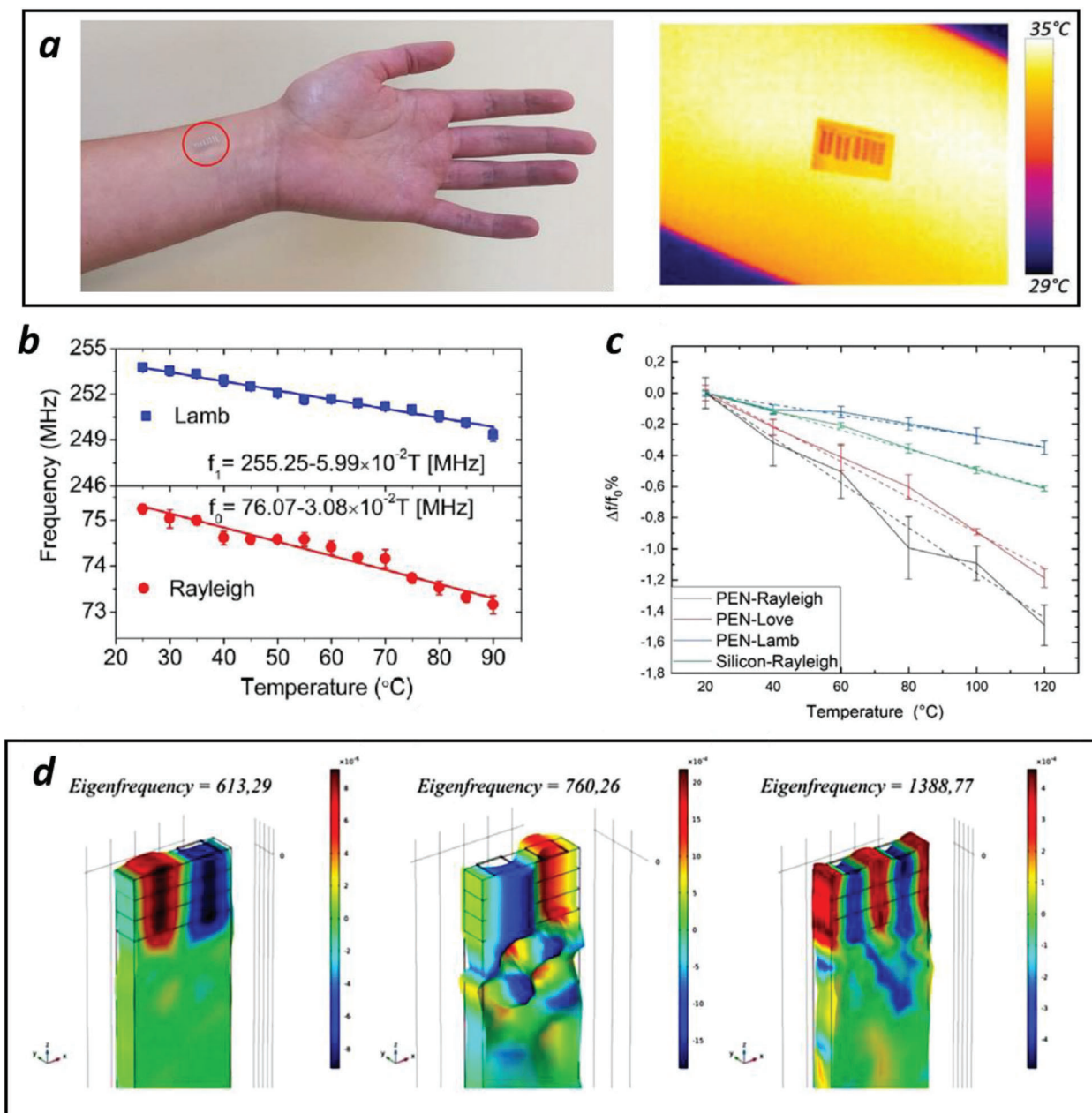


Figure 4. a) Photo of the skin-attached AlN/PEN SAW devices and thermal camera image with the evidence of the uniform heat conduction through the patch from the skin to the SAW device. Reproduced with permission.^[15] Copyright 2019, Wiley-VCH GmbH. b) Working resonance shift as a function of temperature for the Rayleigh and Lamb wave propagating on a ZnO/PI SAW device. Reproduced with permission.^[16] Copyright 2013, Springer Nature. c) Resonance shift % as a function of temperature for the Rayleigh, Love, and Lamb wave propagation on an AlN/PEN SAW device and their comparison with the same device fabricated on a silicon substrate; d) Finite element modeling simulation of superficial eigenfrequency for AlN/PEN device corresponding to the Rayleigh, Shear/Love and Lamb wave propagation, respectively from left to right. Reproduced with permission.^[85] Copyright 2020, Elsevier.

ones, since the polymers have higher thermal expansion. In general, a reduction of the frequency is measured with increasing temperature. The development of flexible polymeric SAW devices paves the way for wearable and wireless temperature sensors based on SAWs (Figure 4a). Jin et al. developed one of the first polymeric SAW devices using ZnO deposited on 100 μm thick Kapton[®],^[16] with two resonance working mode R-SAW at low frequency and (≈ 30 –250 MHz) L-SAW at high frequency

(≈ 150 –500 MHz). They have measured for both the wave modes a linear decrease of the resonance frequency with the temperature increasing, with a TCF of ≈ 442 and, ≈ 245 ppm/ $^{\circ}\text{C}$ for R-SAW and L-SAW respectively (Figure 4b). Years later it has been developed the first polymeric SAW device using AlN, depositing it on 250 μm thick PEN,^[15] measuring TCF of ≈ 810 and ≈ 67 ppm/ $^{\circ}\text{C}$ for the R-SAW at ≈ 250 MHz and L-SAW at ≈ 500 MHz, respectively. Lamanna et al. have developed the first

GHz polymeric-based SAW device working with three different wave modes Rayleigh, Love, and Lamb-like waves (Figure 4c,d). Such devices have been used as temperature sensors showing TCF values of 149, 109, and 53 ppm/°C. Rayleigh and Love wave show higher responsivity to the temperature, with respect to L-SAW, due to the intrinsic nature of such waves. In fact, Rayleigh and Love wave are affected by both piezoelectric and polymeric materials properties since the deformation of such waves fall in both the substrate, how is demonstrated even by finite element modeling (Figure 4d). Lamb-like waves on the contrary travels within the piezoelectric layer and are less affected by the substrate properties. In general, it is known that the TCF is:

$$\text{TCF} \propto \frac{\lambda}{h} \quad (9)$$

where λ is the wavelength and h is the thickness of the piezoelectric layer, with the increasing of such value there is an increase of the TCF. The larger sensitivity to temperature of Rayleigh mode on the flexible substrate is due to the influence of polymeric substrate thermal expansion underneath. In contrast, the Lamb-like waves travel guided within the piezoelectric plate independently of the substrate mechanical properties variation.^[27,28] In many operating conditions, temperature variation can be a significant interference parameter that can invalidate the measurement of other parameters. Therefore, it is common practice to calibrate sensors in an appropriate manner to reduce or eliminate this interference. Zhao et al. conducted an interesting study in this regard, where they developed a strain sensor that can operate at temperatures up to 500 °C.^[90] In their study, the authors considered the thermal expansion coefficient as an added value to the strain variation obtained by the sensor, thereby reducing the error induced by the temperature parameter. This approach effectively minimizes the impact of temperature on the performance of the strain sensor, making it suitable for high-temperature applications.

4.2. Mechanical Sensors

The use of polymeric soft substrate is not just a supplement to the well-established rigid substrate-based electronics but also a key and innovative research field, which opens the door to a variety of applications. In particular, the development of polymeric SAW devices enables the possibility to develop strain/bending sensors based on SAW, impossible with a rigid substrate. The response of the resonance frequency to the deformation is related to a double effect of the strain: a change of the wavelength caused by an IDTs deformation, and the change in the SAWs velocity due to related material properties variation on both piezoelectric layer and polymeric substrate (e.g., density, Young's modulus).^[91,92] Under a compressive strain, the working frequency of the SAW device increases, on the contrary, when stretched a decrease in the resonance frequency is observed. He et al. have developed strain sensors based on ZnO deposited on PET and Polyimide (Figure 5a).^[73,93] The device can withstand deformation of 2500 μe for 100 cycles and up to 3500 μe , higher deformation leads to cracking of the ZnO film and failure of the device. The authors report that the deformation leads to an absolute frequency shift is ≈ 300 kHz when the relative bending strain was changed from

−800 to 1500 μe , at the same time even an insertion loss of −5 dB is observed^[73] (Figure 5b–d). A bending sensor has been developed even with AlN deposited on PEN^[84] measuring curvature angle from −18° to +58° (corresponding to AlN strain of −400 μe / +1000 μe); higher curvature angles lead to the generation of cracks parallel to the bending side. The device has two resonance modes R-SAW and L-SAW both responsive to the deformation, two linear regression slopes, Δf vs strain, of 0.577 kHz/ μe with R^2 and 0.95 and 1.156 kHz/ μe with R^2 0.98 have been obtained for Rayleigh and Lamb modes, respectively (Figure 5e,f). The devices have shown a limit of strain detection of 0.4 and 0.2 μe for the two modes respectively.

Recently, Govindarajan et al. have developed a proof of concept of a strain sensor SAW sensor based on PVDF with remarkable deformation capability 15 800 μe , unfortunately, the system does not allow the development of a calibration curve to define the figure of merit of such sensor^[36] (Figure 5g). The survey confirms the higher sensitivity of the AlN based sensor, which has as drawback its fragility, thus a lower bending capability with respect with ZnO that can detect deformation 2 order of magnitude higher. As concerns the SAW devices based on PVDF, the research is still on fundamental studies and poor in documents. Significant advancements have been made in the development of SAW strain sensors, which leverage thin piezoelectric materials such as Quartz,^[94] Langasite,^[90] and LiNbO₃,^[95] providing a certain degree of bendability. In addition, there are SAW devices based on piezoelectric materials such as ZnO and AlN deposited on thin substrates like aluminum and glass, which also allow for bendability.^[13,14,96] These sensors are increasingly popular as an alternative to polymer-based sensors due to their easy processability. Moreover, they have demonstrated high reliability and can operate at elevated temperatures, making them suitable for various applications.

4.3. Ultraviolet Detectors

UV light is electromagnetic radiation with a wavelength ranging between 10 to 450 nm. Such light has a radical influence on the environment and human survival and development. Excessive exposure to UV is led to cancer and other diseases.^[97] The development of flexible polymeric, low cost and wireless devices to be applied in the monitoring of UV exposure of people, materials and infrastructure is a great challenge and opportunity for MEMS and SAW devices.

The acoustic wave propagation on piezoelectric substrates is accompanied by a traveling potential wave and electric field caused by the polarization of the material due to its deformation, thus the acoustic wave velocity is tied hand in glove with the conductivity of the substrate.^[98,99] Piezoelectric thin films are semiconductors and when illuminated by UV photon, valence band electrons jump into the conduction band to produce free electron-hole pairs, such free carriers will change the electric field resulting in the acoustic wave propagation modulation (Figure 6a). The velocity shift is given by:^[100-103]

$$\frac{\Delta v}{v_0} = \frac{k^2}{2 \left(1 + \left(\frac{\sigma}{\sigma_0} \right)^2 \right)} \quad (10)$$

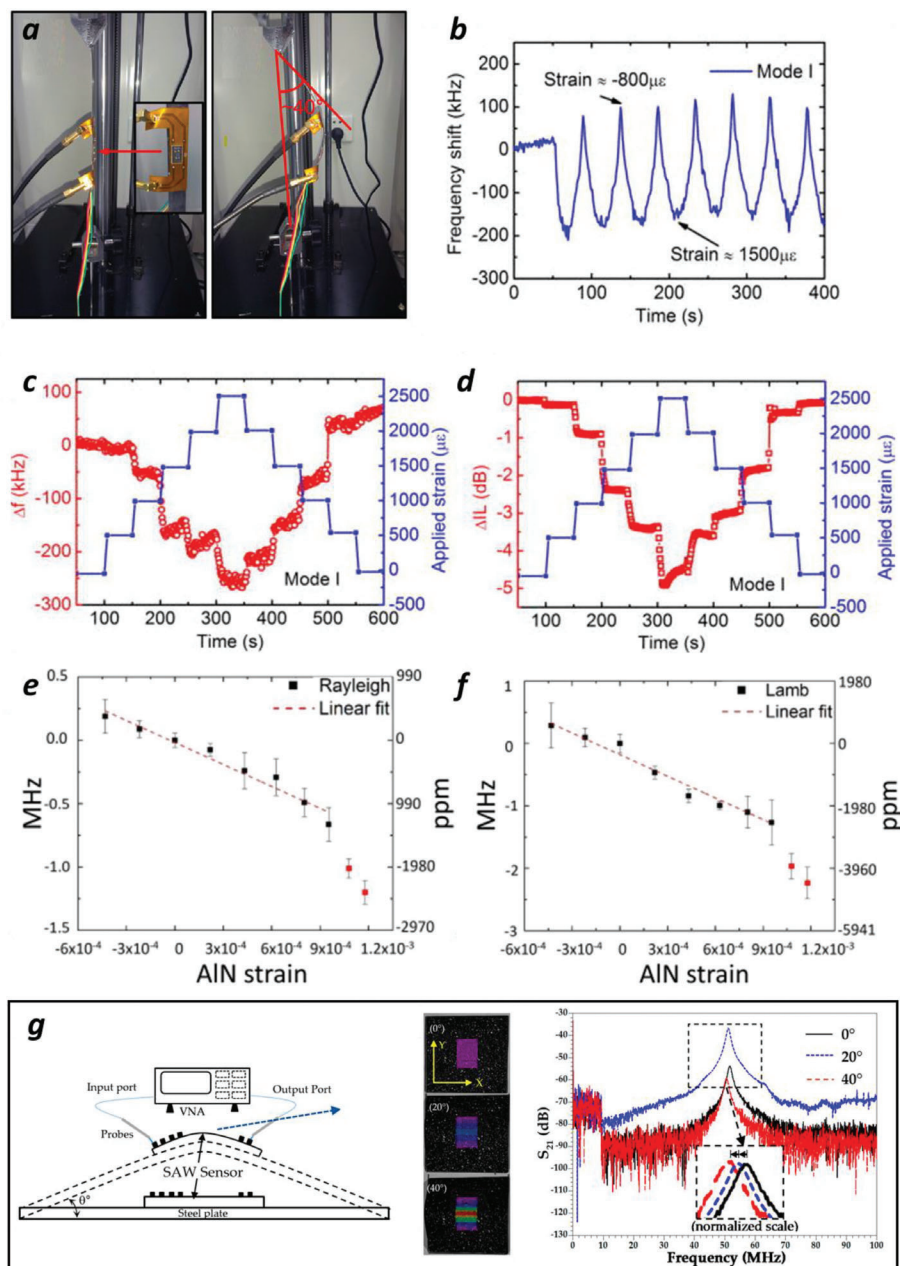


Figure 5. a) Photographs of a ZnO/PET SAW device under bending test; b) Real-time frequency response of the R-SAW devices based on ZnO/PET under strain test (step duration of $t = 46$ s); c,d) Comparison of the frequency and insertion loss response in relation to different strains for ZnO/PET Reproduced with permission.^[73] Copyright 2014, American Institute of Physics. e,f) Resonance frequency shift in function to different strains, for Rayleigh and Lamb modes of devices fabricated on AlN/PEN, respectively. Reproduced with permission.^[84] Copyright 2020, IEEE. g) VNA test setup with PVDF SAW sensor attached to a steel plate bent with angle θ , with related digital image correlation of displacement in Y direction, on the right is reported the frequency response representation from 10 kHz–100 MHz at different angles for PVDF/PZT device. Reproduced under the term of CC-BY license.^[36] Copyright 2021, The Authors, published by MDPI.

where v_0 is the wave velocity, K^2 is the electromechanical coupling coefficient, σ is the sheet conductivity, and σ_m is a material constant. Therefore, the working frequency shift is due to the reduction of the acoustic wave velocity by the increase of photo-induced conductivity of the piezoelectric layer.

ZnO polyimide SAW devices have been characterized using UV light 365 nm at different intensities from 0.4 to

4.5 mW cm⁻². A reduction up to 43 and 76 kHz has been observed for the Rayleigh and Lamb wave respectively, simultaneously with a phase shift of 2.1° and 2.4° for the two modes. At the same time, the authors have observed an amplitude increase due to the insertion loss decreasing, the physics beyond this aspect, observed even in the AlN substrate,^[103] is still not clear and under investigation.^[93] The devices have shown a

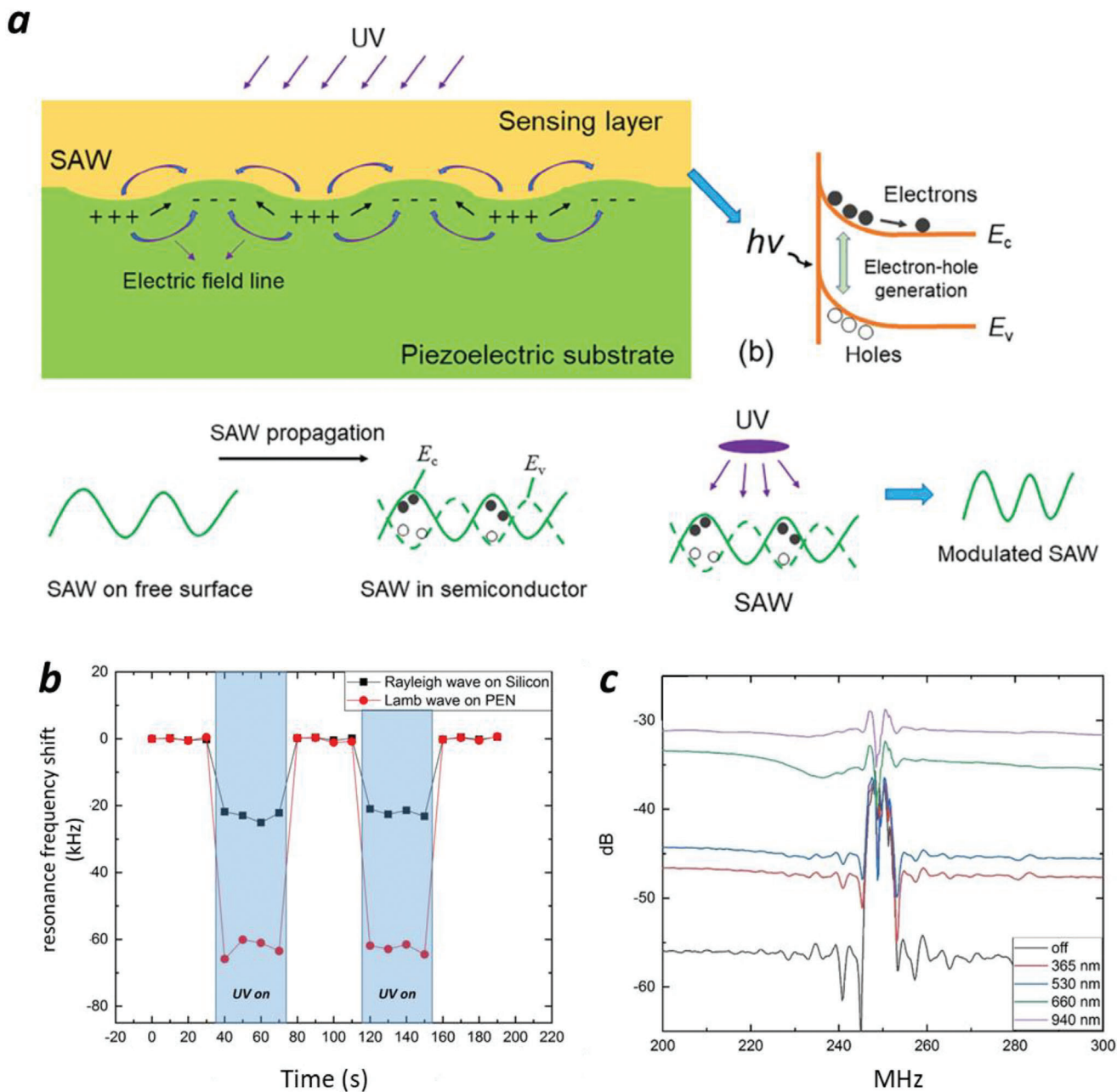


Figure 6. a) Schematics of interactions between SAW propagation on piezoelectric, carriers, and UV light. Reproduced with permission.^[98] Copyright 2020, Elsevier. b) Real-time response of R-SAW on AlN/silicon and L-SAW on AlN/PEN under 365nm LED source. c) Transfer function S_{21} of an AlN/silicon devices irradiated by different wavelengths light. Reproduced with permission.^[103] Copyright 2020, IEEE.

sensitivity of 111.3 and 55.8 ppm/(mW/cm²) for Rayleigh and Lamb wave respectively;^[93] demonstrating higher performance with respect to conventional ZnO devices based on silicon substrate.^[104,105] In general, the high sensitivity of ZnO to UV light has been exploited by depositing nanostructure (pillars, roads) on rigid/metallic SAW devices.^[106] Flexible SAW devices have been developed also exploiting AlN and PEN.^[102,103] AlN has a much higher band gap (≈ 6), with respect to ZnO (≈ 3.2)^[107] that makes the SAW device based on AlN less sensitive to the UV at high wavelengths. However, Lamanna et al. have demonstrated

that the Lamb resonance at 540 MHz undergoes a downshift of ≈ 60 kHz when irradiated with UV at 365 nm 1150 mW, more than twice of AlN/silicon SAW device^[102] (Figure 6b). Moreover, the authors have demonstrated that SAWs on the polymeric substrate were unresponsive to the irradiation at high wavelength. Interestingly the devices fabricated on the silicon substrate were affected by these wavelengths. Silicon has a band gap of 1.14 eV, which is influenced by IR-vis wavelengths leading to an out-of-band insertion loss of the device (Figure 6c). This modulation did not affect the resonance frequency of the SAW

device that on the contrary is defined by the piezoelectric layer properties.^[103] In general, the use of polymeric substrate avoids any influence of the substrate on SAW propagation since such material are unresponsive to the light.

4.4. Biosensors and Microfluidics

Polymeric flexible SAW device finds their natural outgrowth in the development of biosensor and Lab on a chip.^[11,108] Portable, miniaturized, and compliant devices are required not only in healthcare monitoring but even in the food chain, to monitor contamination and food ripening, and even as support for environmental and agriculture monitoring.^[109-111] From this perspective, the development of polymeric SAW devices lags behind conventional SAW devices that have achieved remarkable advancements in recent years. For example, conventional SAW devices have been able to detect various viruses such as Measles,^[111] Influenza,^[112] HIV,^[113] and Ebola,^[114] as well as cancer cells.^[115,116] Furthermore, these devices can even detect biomolecules and protein markers^[117,118] of some pathologies and toxins,^[119,120] in some cases with sub-nanomolar detection limits of 10^{-4} – 10^{-12} M.^[121] In recent years, SAW sensors have also been developed for the detection of DNA or even DNA polymorphisms.^[122-124] These systems commonly employ integrated microfluidic systems, allowing for rapid and accurate detection of various analytes in real-time. SAW devices are frequently utilized for both detection and actuation purposes, including mixing, temperature control, and sorting, among others. Hereafter, an overview of the latest developments in polymeric SAW devices for biosensing applications and their integration into microfluidic systems is presented.

ZnO is hydrophilic material and water molecules are easily absorbed on the piezoelectric layer, leading to the introduction of additional mass that influence the resonance frequency of the SAW device. He et al. developed one of the first humidity sensors based on ZnO growth on polyimide, without any surface treatment or additional sensitive layer.^[125] The work characterized the device from 10% to 80% relative humidity (RH) observing linear regression, without any saturation or hysteresis and with a response time of ≈ 60 s. The sensitivity of the device has been reported as 34.7 kHz/10% RH ≈ 3 times that obtained with rigid SAW sensors with no surface treatment (≈ 13.7 kHz/10% RH),^[126] but smaller than rigid SAW sensors functionalized with absorbent polymers or nanostructure.^[127,128] Xuan et al. developed a flexible SAW humidity sensor by functionalizing ZnO/PI with graphene oxide to exploit its large surface area and high sensitivity to humidity.^[129] The authors demonstrated a sensitivity of up to 145.83 ppm/%RH for both resonance modes in the range of 10%RH to 80%RH (Figure 7a).

AlN, on the contrary, does not absorb water, thus the addition of a sensing layer is necessary to develop a humidity sensor. Piro et al. have developed the first proof of concept of a flexible and wearable SAW microfluidic device for pH detection.^[130] The device consists of a SAW delay line based AlN/PEN, where a microfluidic channel has been microfabricated using SU8 and subsequently functionalized with the ZnO nanoparticles of ≈ 400 nm. The authors demonstrated that such a device can de-

tect pH from 2 to 7 by exploiting the Lamb wave propagation with a sensitivity of ≈ 30 kHz/pH ($R^2 = 0.98$) (Figure 7b); no sensing is reported with the Rayleigh mode.^[130]

Jin et al. have presented an interesting application of polymeric wearable SAW devices based on ZnO and polyimide: a wireless sensor for obstructive sleep apnea syndrome (OSAS).^[131] The authors have compared the obtained results with the ones obtained with conventional LiNbO₃-based SAW sensors. The device was able to monitor in real-time the breathing signal by exploiting the humidity of the exhaled air. The SAW sensor was placed on the upper lip below the nose of a person, and a variation in the humidity of breathing air was detected by the SAW sensor. The authors demonstrated that the shift of the resonance frequency was not particularly suitable for the monitoring of OSAS, on the contrary, the shift in the return loss was successful. The shift of loss caused by respiration was $\approx 0.6 \pm 0.1$ dB, with a response time and recovery of 1.125 and 0.75 s, respectively, shorter than a breathing period. Moreover, the loss recovers to its original value, showing excellent repeatability and stability.

Interaction of SAW with liquids leads to the dissipation of energy and generation of acoustic streaming, pumping, mixing, and even atomization; such dissipation is strictly related to the wave mode and frequency and is usually reported for the R-SAW.^[23] Jin et al. found that even flexible devices based on ZnO and Kapton can provide the same functions.^[16] In particular, the device induces the streaming of drops by the action of R-SAW. The author highlighted an increase in streaming velocity proportional to the droplet dimension and applied voltage, with a maximum of 4 cm s⁻¹ for 10 μ L droplet and an applied voltage of 9.5 V (Figure 7c). The same authors have demonstrated the capability of the device to induce circular streaming to TiO₂ nanoparticle, with the ability to concentrate them at the center of the droplet. Recently Zahertar et al.^[132] have carried out a study evaluating the influence of thin metal layers deposition (Ni/Cu/Ni) on ZnO/PET SAW device performances.^[132] The metal layer enhances the acoustic streaming efficiency, demonstrating pumping actuation with a velocity of 0.52 mm s⁻¹ with a power of 3.6 W, without the presence of such a layer the authors have observed no acoustofluidic function, due to the acoustic energy loss into the polymer layer.

Polymeric SAW devices have been exploited as a biosensor for bacteria detection. Lamanna et al. have developed the first biosensor, based on polymeric PEN and AlN piezoelectric layer, for the detection of *E. Coli*,^[133] one of the most widespread food contaminants. The surface of the device was functionalized with Porten-A/antibody for *E. Coli*, and bovine serum albumin (BSA) for preventing non-specific bonding (Figure 7d). The biosensor exploits the Lamb wave at high frequency proving a Limit of detection of $6.54 \cdot 10^5$ and a limit of saturation at $2.25 \cdot 10^8$ (Figure 7e). The device fabricated on the polymeric substrate have demonstrated figures of merits better than those obtained on the silicon substrate, which cannot exploit the lamb wave at high frequency. Moreover, the development of a FEM and the combination of the real data has allowed the authors to estimate the mass of a single *E. Coli* $\approx 9 \cdot 10^{-13}$ g. The work has demonstrated the high performance of the polymeric SAW device, and its potential application to monitor infection and contamination in food (Figure 7).

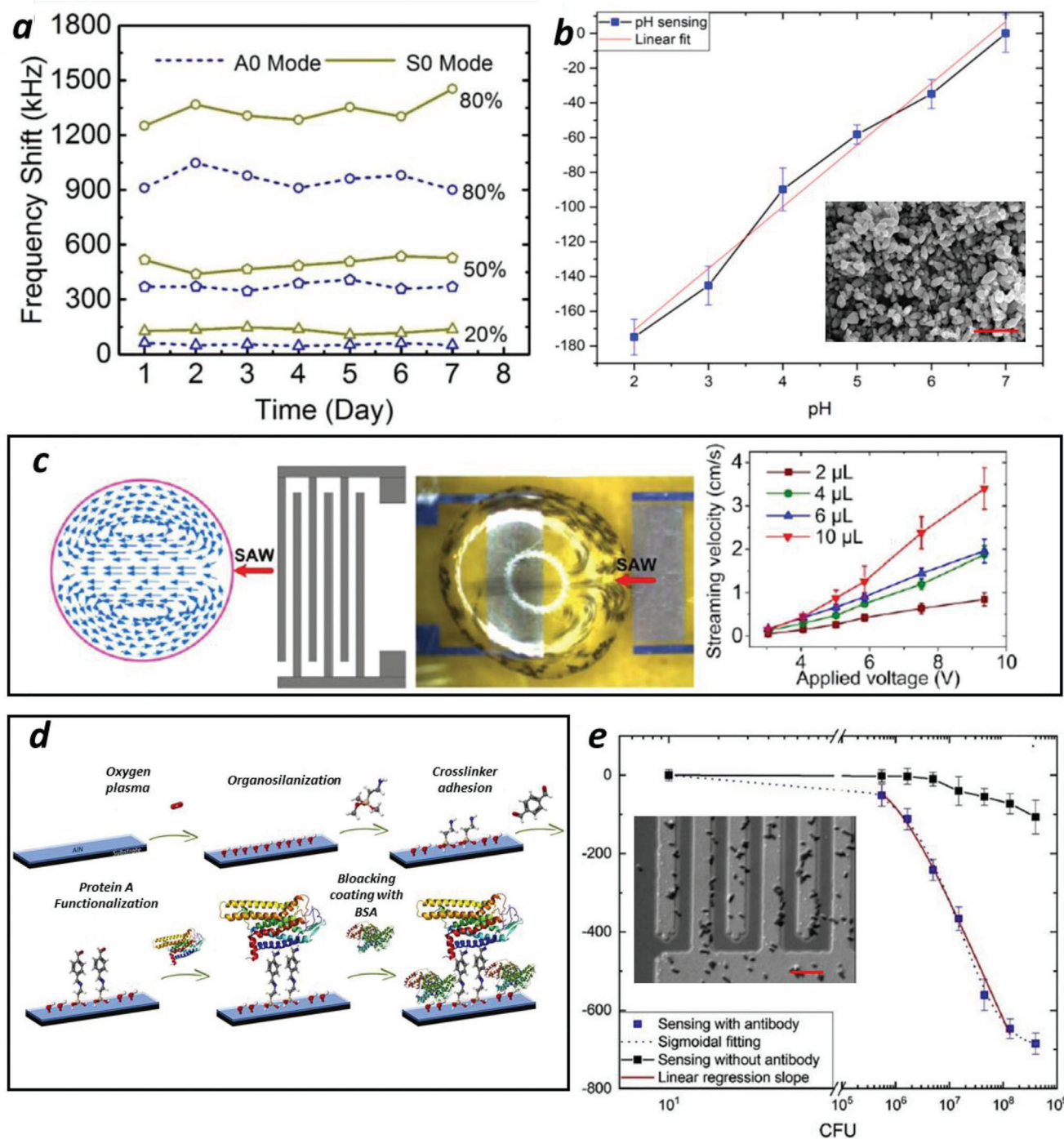


Figure 7. a) Resonant frequency shift is investigated as a function of relative humidity and time for two different modes of flexible ZnO/PI SAW sensors. Reproduced with permission.^[129] Copyright 2015, Elsevier. b) Resonance frequency response to different pH values for an AlN/PEN SAW device functionalized with ZnO nanoparticles. Reproduced under the term of CC-BY license.^[130] Copyright 2021, The Authors, published by MDPI. c) From left to right: a schematic drawing of acoustic streaming inside a liquid droplet, a snapshot of acoustic streaming induced by the flexible ZnO/Kapton SAW device, streaming velocity as a function of RF signal voltage with droplet size as a parameter. Reproduced with permission.^[16] Copyright 2013, Springer Nature; d) Processing steps of surface AlN/PEN SAW device functionalization: i) Hydroxylation using O₂ plasma; ii) Organosilanization with APTES; iii) Surface activation using a crosslinking agent; iii) Protein-A functionalization and blocking coating with BSA; e) Resonance frequency shift as a function of the bacteria concentration, with and without antibody grafting (blue and black respectively L-SAWs on AlN/PEN (inset: SEM imaging of the grafted bacteria). Reproduced with permission.^[133] Copyright 2020, Elsevier.

5. Future Challenges and Trends

The rapid advancements in soft robots, human-machine interfaces, wearables, and edible devices for healthcare are driving the development of new and high-performing materials and components for electronics. In this regard, flexible/polymeric SAW devices represent a promising platform for the advancement of automated and digitized microsystems, offering advantages such as low cost, fast response, reliability, ease of operation, and remote-control capabilities.

The advancements in material science and piezoelectric material deposition processes are driving the rapid growth of these MEMS. Flexible SAW devices have already proven their performance in monitoring various physical and biochemical parameters, such as temperature, UV light, humidity, and bacteria. They have also demonstrated their potential for inducing acoustic streaming and mixing in microfluidic systems. While there is high anticipation for the use of polymeric SAW devices in wearable applications, it is important to note that only a few examples of such usage currently exist, and they are still in the preliminary stages. Moreover, there is currently a lack of data reporting on the wearability and long-term stability of such devices, which are critical factors in their practical application. Therefore, further research and development are necessary to fully assess the feasibility of polymeric SAW devices for wearable device applications.

Despite the promising potential of polymeric SAW devices for various applications, there are still significant challenges that need to be addressed. One of the main challenges is still the deposition of high-crystalline and piezoelectric layers onto the substrate, which is essential for achieving high device sensitivity and reliability. The mismatch in thermal and mechanical performance between the polymeric substrates and the piezoelectric material often lead to decreased device performance and durability. To overcome these challenges, various deposition configurations have been explored, such as multistep and tilted deposition, to improve the quality of the piezoelectric layer on the substrate. In addition, cooling systems have been integrated in the sputtering to minimize the impact of thermal stress on the device. Another approach is to modify the piezoelectric material through doping to enhance its piezoelectric properties. Moreover, developing and investigating new polymeric materials is also essential for improving the performance and versatility of polymeric SAW devices. These new materials should have better compatibility with piezoelectric materials, as well as improved thermal and mechanical properties to enhance the device's durability and sensitivity.

Polymeric substrates are the preferred choice for the development of flexible SAW devices due to their low cost, lightweight, and flexibility. However, as previously mentioned, the deposition of piezoelectric crystalline films on polymeric substrates is a challenging process due to the significant differences in mechanical and thermal properties between the two layers. As an alternative, thin metallic foils such as aluminum^[14,134,135] have emerged as an interesting option for flexible SAW device fabrication offering easy processability thanks to the high thermal resistance, but they also have limitations. For instance, metallic foils have higher costs compared to polymers, low impedance, and are often opaque, limiting their use in applications where transparency is important. Additionally, oxidation can occur over time, com-

promising the performance of the device. Furthermore, metallic foils may not allow for the fabrication of stretchable devices or the propagation of high-frequency L-SAW. Despite these drawbacks, metallic foils can still offer a viable option for certain applications, and ongoing research is exploring ways to overcome these limitations.

PVDF (polyvinylidene fluoride) has the potential to be a game-changer in the development of fully organic and flexible/stretchable SAW devices. The low-cost, ease of processing and excellent mechanical and electrical properties of PVDF make it an attractive option for SAW devices. In addition to PVDF, recent studies have reported the piezoelectric properties of biopolymers such as cellulose and chitosan,^[136,137] which have yet to be fully explored for SAW devices. These materials are biocompatible, renewable, and biodegradable, making them attractive for use in biomedical and environmental applications. While their piezoelectric properties are not as strong as those of synthetic polymers, they have shown promise in certain applications. While more research is needed to fully understand the potential of biopolymers for SAW devices, their unique properties make them a promising area of study for the future of flexible and organic SAW devices.

Acknowledgements

The author expresses sincere gratitude to Dr. Francesco Rizzi for the extensive discussions that not only supported but also intensified the author's interest in SAW technology. Without his valuable insights and guidance, this review would not have been possible.

Conflict of Interest

The authors declare no conflict of interest.

Keywords

acoustic devices, AIN, depositions, flexible electronics, sensors, thin films, ZnO

Received: March 7, 2023

Revised: May 4, 2023

Published online: August 15, 2023

- [1] R. Crabb, F. Treble, *Nature* **1967**, 213, 1223.
- [2] I. Kymissis, Wiley Online Library, **2018**.
- [3] W. A. MacDonald, *Large Area and Flexible Electronics* **2015**, 291.
- [4] J. A. Rogers, T. Someya, Y. Huang, *Science* **2010**, 327, 1603.
- [5] L. Lamanna, G. Pace, I. K. Ilic, P. Cataldi, F. Viola, M. Friuli, V. Galli, C. Demitri, M. Caironi, *Nano Energy* **2023**, 108, 108168.
- [6] D. B. Go, M. Z. Atashbar, Z. Ramshani, H.-C. Chang, *Anal. Methods* **2017**, 9, 4112.
- [7] C. Campbell, *Surface Acoustic Wave Devices for Mobile and Wireless Communications, Four-Volume Set*, Academic Press, **1998**.
- [8] B. Liu, X. Chen, H. Cai, M. M. Ali, X. Tian, L. Tao, Y. Yang, T. Ren, *J. Semicond.* **2016**, 37, 021001.
- [9] P. Delsing, A. N. Cleland, M. J. Schuetz, J. Knörzer, G. Giedke, J. I. Cirac, K. Srinivasan, M. Wu, K. C. Balram, C. Bäuerle, *J. Phys. D: Appl. Phys.* **2019**, 52, 353001.

- [10] I. Marasco, G. Niro, L. Lamanna, L. Piro, F. Guido, L. Algieri, V. Mastronardi, A. Qualtieri, E. Scarpa, D. Desmaële, *Microelectron. Eng.* **2020**, 227, 111322.
- [11] M. Agostini, F. Lunardelli, M. Gagliardi, A. Miranda, L. Lamanna, A. G. Luminare, F. Gambineri, M. Lai, M. Pistello, M. Cecchini, *Adv. Funct. Mater.* **2022**, 32, 2201958.
- [12] G. Niro, I. Marasco, L. Lamanna, F. Rizzi, A. D'Orazio, M. de Vittorio, M. Grande, presented at *Microwave Mediterranean Symposium (MMS)*, **2022**.
- [13] J. Wu, C. Yin, J. Zhou, H. Li, Y. Liu, Y. Shen, S. Garner, Y. Fu, H. Duan, *ACS Appl. Mater. Interfaces* **2020**, 12, 39817.
- [14] Y. Wang, Q. Zhang, R. Tao, J. Xie, P. Canyelles-Pericas, H. Torun, J. Reboud, G. McHale, L. E. Dodd, X. Yang, *ACS Appl. Mater. Interfaces* **2021**, 13, 16978.
- [15] L. Lamanna, F. Rizzi, F. Guido, L. Algieri, S. Marras, V. M. Mastronardi, A. Qualtieri, M. De Vittorio, *Adv. Electron. Mater.* **2019**, 5, 1900095.
- [16] H. Jin, J. Zhou, X. He, W. Wang, H. Guo, S. Dong, D. Wang, Y. Xu, J. Geng, J. Luo, *Sci. Rep.* **2013**, 3, 2140.
- [17] X. Peng, K. Dong, Z. Wu, J. Wang, Z. L. Wang, *J. Mater. Sci.* **2021**, 56, 16765.
- [18] W. B. Han, J. H. Lee, J. W. Shin, S. W. Hwang, *Adv. Mater.* **2020**, 32, 2002211.
- [19] H. Ling, S. Liu, Z. Zheng, F. Yan, *Small Methods* **2018**, 2, 1800070.
- [20] Y. Huang, E.-L. Hsiang, M.-Y. Deng, S.-T. Wu, *Light: Sci. Appl.* **2020**, 9, 105.
- [21] I. K. Ilic, V. Galli, L. Lamanna, P. Cataldi, L. Pasquale, V. F. Annese, A. Athanassiou, M. Caironi, *Adv. Mater.* **2023**, 35, 2211400.
- [22] A. S. Sharova, M. Caironi, *Adv. Mater.* **2021**, 33, 2103183.
- [23] Y. Q. Fu, J. Luo, N.-T. Nguyen, A. Walton, A. J. Flewitt, X.-T. Zu, Y. Li, G. McHale, A. Matthews, E. Iborra, *Prog. Mater. Sci.* **2017**, 89, 31.
- [24] L. Rayleigh, *Proceedings of the London Mathematical Society* **1885**, 1, 4.
- [25] M. Rahman, T. Michelitsch, *Wave Motion* **2006**, 43, 272.
- [26] P. Aryan, A. Kotousov, C. Ng, B. Cazzolato, **2014**.
- [27] H. Lamb, *Proc. R. Soc. Lond. A* **1917**, 93, 114.
- [28] J. Achenbach, *Wave propagation in elastic solids*, Vol. 16, Elsevier, **2012**.
- [29] S. Bruckenstein, M. Shay, *Electrochim. Acta* **1985**, 30, 1295.
- [30] M. Bharati, L. Rana, M. Tomar, V. Gupta, *Materials Today: Proceedings* **2021**, 47, 1538.
- [31] N. V. Ramachandran, **2018**.
- [32] K. S. Ramadan, D. Sameoto, S. Evoy, *Smart Mater. Struct.* **2014**, 23, 033001.
- [33] R. S. Wagers, presented at *1979 Ultrasonics Symposium*, **1979**.
- [34] R. Wagers, *J. Appl. Phys.* **1980**, 51, 5797.
- [35] A. Kumar, G. Thachil, S. Dutta, *Sens. Actuators, A* **2019**, 292, 52.
- [36] R. Srinivasaraghavan Govindarajan, E. Rojas-Nastrucci, D. Kim, *Crystals* **2021**, 11, 1576.
- [37] Ü. Özgür, Y. I. Alivov, C. Liu, A. Teke, M. Reshchikov, S. Doğan, V. Avrutin, S.-J. Cho, H. Morkoç, *J. Appl. Phys.* **2005**, 98, 11.
- [38] M. A. Borysiewicz, *Crystals* **2019**, 9, 505.
- [39] Y. Yoshino, *J. Appl. Phys.* **2009**, 105, 061623.
- [40] L. Fan, S.-y. Zhang, H. Ge, H. Zhang, *J. Appl. Phys.* **2013**, 114, 024504.
- [41] D.-T. Phan, G.-S. Chung, *J. Electroceram.* **2013**, 30, 185.
- [42] G. Cong, H. Wei, P. Zhang, W. Peng, J. Wu, X. Liu, C. Jiao, W. Hu, Q. Zhu, Z. Wang, *Appl. Phys. Lett.* **2005**, 87, 231903.
- [43] U. C. Kaletta, C. Wipf, M. Fraschke, D. Wolansky, M. A. Schubert, T. Schroeder, C. Wenger, *IEEE Trans. Electron Devices* **2015**, 62, 764.
- [44] R. M. Pinto, V. Gund, C. Calaza, K. Nagaraja, K. Vinayakumar, *Microelectron. Eng.* **2022**, 257, 111753.
- [45] T. Aubert, J. Bardong, O. Legrani, O. Elmazria, M. Badreddine Assouar, G. Bruckner, A. Talbi, *J. Appl. Phys.* **2013**, 114, 014505.
- [46] K.-T. Yong, S. F. Yu, *J. Mater. Sci.* **2012**, 47, 5341.
- [47] A. Artieda, M. Barbieri, C. S. Sandu, P. Murali, *J. Appl. Phys.* **2009**, 105, 024504.
- [48] X.-H. Xu, H.-S. Wu, C.-J. Zhang, Z.-H. Jin, *Thin Solid Films* **2001**, 388, 62.
- [49] E. L. Bedia, S. Murakami, T. Kitade, S. Kohjiya, *Polymer* **2001**, 42, 7299.
- [50] V. R. Sastri, *Plast Med Devices* (Eds: VR. Sastri), William Andrew Publishing, Oxford, UK **2014**, 173.
- [51] O. Serbanescu, S. Voicu, V. Thakur, *Materials Today Chemistry* **2020**, 17, 100302.
- [52] E. Dhanumalayan, G. M. Joshi, *Adv. Compos. Hyb. Mater.* **2018**, 1, 247.
- [53] R. Weber, A. Watson, M. Forter, F. Oliaei, *Waste Manag. Res.* **2011**, 29, 107.
- [54] T. Kumada, M. Ohtsuka, H. Fukuyama, *AIP Adv.* **2015**, 5, 017136.
- [55] C. Caliendo, P. Imperatori, *J. Appl. Phys.* **2004**, 96, 2610.
- [56] K. Sundaram, A. Khan, *Thin Solid Films* **1997**, 295, 87.
- [57] J. P. Atanas, R. Al Asmar, A. Khoury, A. Foucaran, *Sens. Actuators, A* **2006**, 127, 49.
- [58] A. Szekeres, Z. Fogarassy, P. Petrik, E. Vlaikova, A. Cziraki, G. Socol, C. Ristoscu, S. Grigorescu, I. Mihailescu, *Appl. Surf. Sci.* **2011**, 257, 5370.
- [59] M. Matsumura, R. P. Camata, *Thin Solid Films* **2005**, 476, 317.
- [60] D. C. Look, D. Reynolds, C. Litton, R. Jones, D. Eason, G. Cantwell, *Appl. Phys. Lett.* **2002**, 81, 1830.
- [61] Y. Kim, J. Lee, Y. Noh, J. Oh, S. Ahn, *Thin Solid Films* **2015**, 576, 61.
- [62] Y. Xi, K. Chen, F. Mont, J. Kim, E. Schubert, C. Wetzel, W. Liu, X. Li, J. Smart, *J. Electron. Mater.* **2007**, 36, 533.
- [63] F. Huber, M. Madel, A. Reiser, S. Bauer, K. Thonke, *J. Cryst. Growth* **2016**, 445, 58.
- [64] W. Ostachowicz, P. Kudela, M. Krawczuk, A. Zak, *Guided waves in structures for SHM: the time-domain spectral element method*, John Wiley & Sons, **2011**.
- [65] E. Smecca, F. Maita, G. Pellegrino, V. Vinciguerra, L. La Magna, S. Mirabella, L. Maiolo, G. Fortunato, G. G. Condorelli, A. Alberti, *Appl. Phys. Lett.* **2015**, 106, 232903.
- [66] R. Tait, A. Mirfazli, *J. Vac. Sci. Technol., A* **2001**, 19, 1586.
- [67] S. Amara, F. Kanouni, F. Laidoudi, K. Bouamama, *Phys. B* **2021**, 615, 412990.
- [68] J.-B. Lee, H.-J. Lee, S.-H. Seo, J.-S. Park, *Thin Solid Films* **2001**, 398, 641.
- [69] J. Zhou, X. L. He, W. B. Wang, Q. Zhu, W. P. Xuan, H. Jin, S. R. Dong, M. De Wang, J. K. Luo, *IEEE Electron Device Lett.* **2013**, 34, 1319.
- [70] F. Kanouni, L. Farouk, presented at *IEEE International Meeting for Future of Electron Devices*, Kansai Japan, **2022**.
- [71] J. Zhou, X. He, H. Jin, W. Wang, B. Feng, S. Dong, D. Wang, G. Zou, J. Luo, *J. Appl. Phys.* **2013**, 114, 044502.
- [72] Q. Li, H. Liu, G. Li, F. Zeng, F. Pan, J. Luo, L. Qian, *J. Electron. Mater.* **2016**, 45, 2702.
- [73] X. He, H. Guo, J. Chen, W. Wang, W. Xuan, Y. Xu, J. Luo, *Appl. Phys. Lett.* **2014**, 104, 213504.
- [74] H. R. Choi, S. K. Eswaran, Y. S. Cho, *ACS Appl. Mater. Interfaces* **2015**, 7, 14654.
- [75] H. S. Min, M. K. Yang, J.-K. Lee, *J. Vac. Sci. Technol., A* **2009**, 27, 352.
- [76] K. Chen, K. S. Chiang, H. P. Chan, P. L. Chu, *Optical Materials* **2008**, 30, 1244.
- [77] Y.-y. Liu, Y.-I. Zang, G.-x. Wei, J. Li, X.-L. Fan, C.-f. Cheng, *Mater. Lett.* **2009**, 63, 2597.
- [78] Y.-y. Liu, Y.-z. Yuan, X.-t. Gao, S.-s. Yan, X.-z. Cao, G.-x. Wei, *Mater. Lett.* **2007**, 61, 4463.
- [79] N. Jackson, L. Keeney, A. Mathewson, *Smart Mater. Struct.* **2013**, 22, 115033.

- [80] S. Petroni, G. Maruccio, F. Guido, M. Amato, A. Campa, A. Passaseo, M. Todaro, M. De Vittorio, *Microelectron. Eng.* **2012**, *98*, 603.
- [81] V. M. Mastronardi, F. Guido, M. Amato, M. De Vittorio, S. Petroni, *Microelectron. Eng.* **2014**, *121*, 59.
- [82] J. Zhou, S. Dong, H. Jin, B. Feng, D. Wang, *J. Cont. Sci. Engin.* **2012**, *2012*, 5.
- [83] K. Li, F. Wang, M. Deng, K. Hu, D. Song, Y. Hao, H. Di, K. Dong, S. Yan, Z. Song, *J. Mater. Sci.: Mater. Electron.* **2021**, *32*, 13146.
- [84] L. Lamanna, F. Rizzi, F. Giudo, M. De Vittorio, *IEEE Electron Device Lett.* **2020**, *41*, 1692.
- [85] L. Lamanna, F. Rizzi, V. R. Bhethanabotla, M. De Vittorio, *Sens. Actuators, A* **2020**, 112268.
- [86] L. Lu, W. Ding, J. Liu, B. Yang, *Nano Energy* **2020**, *78*, 105251.
- [87] P. Ueberschlag, *Sensor Rev.* **2001**, *21*, 118.
- [88] L. Wu, Z. Jin, Y. Liu, H. Ning, X. Liu, N. Hu, *Nanotechnology Reviews* **2022**, *11*, 1386.
- [89] I. Gouzman, E. Grossman, R. Verker, N. Atar, A. Bolker, N. Eliaz, *Adv. Mater.* **2019**, *31*, 1807738.
- [90] J. Zhang, H. Jin, S. Dong, R. Ding, J. Chen, W. Xuan, F. Gao, J. Luo, *IEEE Sens. J.* **2022**, *22*, 11509.
- [91] H. Spetzler, R. Martin, *Nature* **1974**, *252*, 30.
- [92] F. Rawson, J. Rider, *Polymer* **1974**, *15*, 107.
- [93] X. He, J. Zhou, W. Wang, W. Xuan, X. Yang, H. Jin, J. Luo, *J. Micromech. Microeng.* **2014**, *24*, 055014.
- [94] B. Feng, H. Jin, Z. Fang, Z. Yu, S. Dong, J. Luo, *IEEE Sens. J.* **2021**, *21*, 18571.
- [95] H. Xu, S. Dong, W. Xuan, U. Farooq, S. Huang, M. Li, T. Wu, H. Jin, X. Wang, J. Luo, *Appl. Phys. Lett.* **2018**, *112*, 093502.
- [96] R. Tao, W. Wang, J. Luo, S. A. Hasan, H. Torun, P. Canyelles-Pericas, J. Zhou, W. Xuan, M. Cooke, D. Gibson, *Surf. Coat. Technol.* **2019**, *357*, 587.
- [97] D. L. Narayanan, R. N. Saladi, J. L. Fox, *Internat. J. Dermat.* **2010**, *49*, 978.
- [98] Y. Zhang, Y. Cai, J. Zhou, Y. Xie, Q. Xu, Y. Zou, S. Guo, H. Xu, C. Sun, S. Liu, *Sci. Bull.* **2020**, *65*, 587.
- [99] A. Wixforth, J. Scriba, M. Wassermeier, J. P. Kotthaus, G. Weimann, W. Schlapp, *Phys. Rev. B* **1989**, *40*, 7874.
- [100] M. Rotter, A. Wixforth, W. Ruile, D. Bernklau, H. Riechert, *Appl. Phys. Lett.* **1998**, *73*, 2128.
- [101] S. Wang, Z.-J. Li, X. Zhou, C. Zhao, X.-T. Zu, Y. Q. Fu, *Nanosci. Nanotech. Letters* **2015**, *7*, 169.
- [102] L. Lamanna, F. Rizzi, M. De Vittorio, V. R. Bhethanabotla, *2019 IEEE Sensors, IEEE* **2019**, 1.
- [103] L. Lamanna, F. Rizzi, M. Bianco, M. Agostini, M. Cecchini, M. De Vittorio, V. R. Bhethanabotla, *IEEE Sens. J.* **2020**, *21*, 9675.
- [104] P. Sharma, K. Sreenivas, *Appl. Phys. Lett.* **2003**, *83*, 3617.
- [105] W.-S. Wang, T.-T. Wu, presented at *IEEE International Frequency Control Symposium*, **2010**.
- [106] S. A. Hasan, H. Torun, D. Gibson, Q. Wu, M. D. Cooke, Y. Fu, presented at *IEEE Jordan International Joint Conference on Electrical Engineering and Information Technology (JEEIT)*, **2019**.
- [107] E. Lee, J. Park, M. Yim, Y. Kim, G. Yoon, *Appl. Phys. Lett.* **2015**, *106*, 023901.
- [108] M. Gagliardi, M. Agostini, F. Lunardelli, L. Lamanna, A. Miranda, A. Bazzichi, A. G. Luminare, F. Cervelli, F. Gambineri, M. Totaro, *Sens. Actuators, B* **2023**, *379*, 133299.
- [109] P. Cataldi, L. Lamanna, C. Bertei, F. Arena, P. Rossi, M. Liu, F. Di Fonzo, D. G. Papageorgiou, A. Luzio, M. Caironi, *Adv. Funct. Mater., n/a*, 2113417.
- [110] I. K. Ilic, L. Lamanna, D. Cortecchia, P. Cataldi, A. Luzio, M. Caironi, *ACS Sens.* **2022**, *7*, 2995.
- [111] L. Lamanna, P. Cataldi, M. Friuli, C. Demitri, M. Caironi, *Adv. Mater. Technol.* **2022**, *8*, 2200731.
- [112] Y. Jiang, C. Y. Tan, S. Y. Tan, M. S. F. Wong, Y. F. Chen, L. Zhang, K. Yao, S. K. E. Gan, C. Verma, Y.-J. Tan, *Sens. Actuators, B* **2015**, *209*, 78.
- [113] E. R. Gray, V. Turbé, V. E. Lawson, R. H. Page, Z. C. Cook, R. B. Ferns, E. Nastouli, D. Pillay, H. Yatsuda, D. Athey, *NPJ Digital Medicine* **2018**, *1*, 35.
- [114] J. T. Baca, V. Severns, D. Lovato, D. W. Branch, R. S. Larson, *Sensors* **2015**, *15*, 8605.
- [115] K. Chang, Y. Pi, W. Lu, F. Wang, F. Pan, F. Li, S. Jia, J. Shi, S. Deng, M. Chen, *Biosens. Bioelectron.* **2014**, *60*, 318.
- [116] K. Wang, W. Zhou, Z. Lin, F. Cai, F. Li, J. Wu, L. Meng, L. Niu, H. Zheng, *Sens. Actuators, B* **2018**, *258*, 1174.
- [117] S. Li, Y. Wan, Y. Su, C. Fan, V. R. Bhethanabotla, *Biosens. Bioelectron.* **2017**, *95*, 48.
- [118] P. Jandas, J. Luo, A. Quan, C. Qiu, W. Cao, C. Fu, Y. Q. Fu, *Appl. Surf. Sci.* **2020**, *518*, 146061.
- [119] X. Zhang, J. Fang, L. Zou, Y. Zou, L. Lang, F. Gao, N. Hu, P. Wang, *Biosens. Bioelectron.* **2016**, *77*, 573.
- [120] J. Ji, Y. Pang, D. Li, Z. Huang, Z. Zhang, N. Xue, Y. Xu, X. Mu, *Microsyst. Nanoeng.* **2020**, *6*, 4.
- [121] M. Agostini, G. Greco, M. Cecchini, *Sens. Actuators, B: Chem.* **2018**, *254*, 1.
- [122] H.-L. Cai, Y. Yang, X. Chen, M. A. Mohammad, T.-X. Ye, C.-R. Guo, L.-T. Yi, C.-J. Zhou, J. Liu, T.-L. Ren, *Biosens. Bioelectron.* **2015**, *71*, 261.
- [123] Y. Zhang, F. Yang, Z. Sun, Y.-T. Li, G.-J. Zhang, *Analyst* **2017**, *142*, 3468.
- [124] N. Fourati, M. Lazerges, C. Vedrine, J.-M. Fournion, C. Zerrouki, L. Rousseau, P. Lepeut, J. J. Bonnet, C. Pernelle, *Sensor Letters* **2009**, *7*, 847.
- [125] X. He, D. Li, J. Zhou, W. Wang, W. Xuan, S. Dong, H. Jin, J. Luo, *J. Mater. Chem. C* **2013**, *1*, 6210.
- [126] C. Caliendo, E. Verona, V. Anisimkin, *Smart Mater. Struct.* **1997**, *6*, 707.
- [127] T.-T. Wu, Y.-Y. Chen, T.-H. Chou, *J. Phys. D: Appl. Phys.* **2008**, *41*, 085101.
- [128] H.-S. Hong, D.-T. Phan, G.-S. Chung, *Sens. Actuators, B* **2012**, *171*, 1283.
- [129] W. Xuan, J. Chen, X. He, W. Wang, S. Dong, J. Luo, *Proc. Eng.* **2015**, *120*, 364.
- [130] L. Piro, L. Lamanna, F. Guido, A. Balena, M. Mariello, F. Rizzi, M. De Vittorio, *Nanomaterials* **2021**, *11*, 1479.
- [131] H. Jin, X. Tao, S. Dong, Y. Qin, L. Yu, J. Luo, M. J. Deen, *J. Micromech. Microeng.* **2017**, *27*, 115006.
- [132] S. Zahertar, R. Tao, H. Wang, H. Torun, P. Canyelles-Pericas, Y. Liu, J. Vernon, W. P. Ng, R. Binns, Q. Wu, *IEEE Sens. J.* **2022**, *1*.
- [133] L. Lamanna, F. Rizzi, V. R. Bhethanabotla, M. De Vittorio, *Biosens. Bioelectron.* **2020**, *163*, 112164.
- [134] S. Maramizonouz, X. Tao, M. Rahmati, C. Jia, R. Tao, H. Torun, T. Zheng, H. Jin, S. Dong, J. Luo, *Inter. J. Mechan. Sci.* **2021**, *202*, 106536.
- [135] Q. Zhang, Y. Wang, D. Li, X. Yang, J. Xie, Y. Fu, *Appl. Phys. Lett.* **2021**, *118*, 121601.
- [136] Y. Song, Z. Shi, G.-H. Hu, C. Xiong, A. Isogai, Q. Yang, *J. Mater. Chem. A* **2021**, *9*, 1910.
- [137] G. de Marzo, V. M. Mastronardi, L. Algieri, F. Vergari, F. Pisano, L. Fachechi, S. Marras, L. Natta, B. Spagnolo, V. Brunetti, *Adv. Electron. Mater.* **2022**, 2200069.



Leonardo Lamanna is a researcher at Università del Salento, specializing in Engineering of Materials and Nanotechnology. He holds a Ph.D. from the same university and completed a scholar research program at the University of South Florida. With a background in experimental research, he worked at Gelesis on optimizing hydrogels for weight management. During his postdoctoral research in Pisa and Milan, he focused on wearables and edible devices, exploring new technology and wireless communication strategies. His research centers on novel materials, technology, and devices for emerging fields, reflecting a strong interest in advancing these areas.